

results strongly dependent on the details of the individual scattering elements and the electrical parameters of the matrix of material in which the scatterers are "suspended." The most fundamental example for which an analytical solution is known is the case of isotropic scattering in a semi-infinite, plane parallel half space [6]. The assumptions of this theory are important, of course. It assumes that radiation incident on a scatterer is uniformly scattered in all directions. For this to be strictly true, electromagnetic theory requires that the scatterers be ellipsoidal with random orientations and be separated by distances long compared to the wavelength in the medium. Chandrasaker's solution intrinsically assumes that the scatterers are suspended in a transparent medium. The ideas were adopted in [3] with the argument that rocks in light venusian soils may behave this way to first order on average, even though the scatterers are probably far from spherical and may be piled on top of each other. The fact that the matrix supporting the scatterers is not completely transparent is not serious as long as it is sufficiently transparent to allow the radiation to scatter a "few" times before absorption or before the energy is backscattered out of the layer.

If we visualize the scatterers as rocks and fragments we may consider a suite of likely models that would display the microwave observables seen in the PV and Magellan data. Such rocks would exist at all sizes from dust to the rare boulders of many meters. It is reasonable to assume that the particle sizes could be represented by a power law distribution and a good guess at the slope parameter of the distribution would be about -3 , consistent with that found from tumbling rocks in a fracturing process. The index is not of great importance. We assume that the soil matrix has a real dielectric constant of 2, consistent with the flat regions on Venus that exhibit the lowest reflectivity. Such soils would have densities under 1 gm/cm^3 and power absorption lengths of order $2-3 \text{ m}$. The rocks would have dielectric constants in the range of $5-8$, primarily dependent on the metal content, and corresponding absorption lengths of about $0.6-0.1 \text{ m}$. Silicate rocks have low complex dielectric constants and mafic rocks such as basalts high in Fe have large values. We have applied the theory from [3] to a typical granite and a typical basalt and the resulting 13-cm reflectivities and emissivities at normal incidence are shown in Table 1. An important unknown parameter is the largest size cutoff of the power law size distribution. Obviously, if the "particles" could be as large as kilometers, the results would degenerate to the parameters of the largest sphere and scattering would not be important. The results are presented in the table as a function of the cutoff radius of the size distribution.

TABLE 1.

	Maximum Radius (cm)	Reflectivity	Emissivity
Granite	5	0.617	0.355
	10	0.496	0.486
	30	0.383	0.599
	50	0.341	0.637
	100	0.291	0.679
Basalt	5	0.486	0.509
	10	0.386	0.581
	30	0.304	0.664
	50	0.273	0.690
	100	0.245	0.728

It is clear that this explanation is sufficient for the Venus anomalous features. Furthermore, the parameters approach the average values of the Venus surface when the value of the maximum particle size is increased moderately. There are ambiguities in these calculations, but the ambiguities are intrinsic to the Magellan measurements themselves in rough, heterogeneous areas on Venus where the Hagfors' assumptions are severely bent. New scattering theories involving Monte Carlo techniques will be presented.

References: [1] Pettingill G. H. et al. (1988) *JGR*, 93, 14885. [2] Klose K. et al. (1992) *JGR*, special Magellan issue. [3] Tryja K. and Muhleman D. O. (1992) *JGR*, special Magellan issue. [4] Muhleman D. et al. (1979) *Ap. J.*, 234, 1979. [5] Muhleman D. and Berge G. (1991) *Icarus*, 93, 263. [6] Chandrasaker S., *Radiative Transfer*, Dover Publications.

N93-14350

THE GABBRO-ECLOGITE PHASE TRANSITION AND THE ELEVATION OF MOUNTAIN BELTS ON VENUS. Noriyuki Namiki and Sean C. Solomon, Department of Earth, Atmospheric, and Planetary Sciences, Massachusetts Institute of Technology, Cambridge MA 02139, USA.

Introduction: The linear mountain belts of Ishtar Terra on Venus are notable for their topographic relief and slope and for the intensity of surface deformation [1,2]. The mountains surround the highland plain Lakshmi Planum. Volcanism is rare to absent in Maxwell, Freyja, and Akna Montes, but a number of magmatic features are evident in Danu Montes [2,3], the mountain range least elevated above Lakshmi Planum. Whether western Ishtar Terra is a site of mantle upwelling and consequent hot spot volcanism [4-6] or of mantle downwelling and consequent convergence of lithospheric blocks [7,8] is currently a matter of debate. However, the mountains are generally regarded as products of large-scale compression of the crust and lithosphere [2,9].

Among the four mountain belts surrounding Lakshmi Planum, Maxwell Montes is the highest and stands up to 11 km above the mean planetary radius and 7 km above Lakshmi Planum. The bulk composition and radioactive heat production of the crust on Venus, where measured, are similar to those of terrestrial tholeiitic basalt [10]. Because the thickness of the low-density crust may be limited by the gabbro-garnet granulite-eclogite phase transitions (Fig. 1), the 7-11-km maximum elevation of Maxwell Montes is difficult to understand except in the unlikely situation that the crust contains a large volume of magma [11]. A possible explanation is that the base of the crust is not in phase equilibrium. It has been suggested that under completely dry conditions, the gabbro-eclogite phase transition takes place by solid-state diffusion and may require a geologically significant time to run to completion [12]. Solid-state diffusion is a strongly temperature-dependent process. In this paper we solve the thermal evolution of the mountain belt to attempt to constrain the depth of the gabbro-eclogite transition and thus to assess this hypothesis quantitatively.

Thermal Model: The one-dimensional heat equation is solved numerically by a finite difference approximation. The deformation of the horizontally shortening crustal and mantle portions of the thermal boundary layer is assumed to occur by pure shear, and therefore the vertical velocity is given by the product of the horizontal strain rate $\dot{\gamma}$ and depth z . The thermal diffusivity is assumed to be $1.0 \times 10^{-6} \text{ m}^2 \text{ s}^{-1}$ in both crust and mantle. Crustal heat production is assumed to equal $1.4 \times 10^{-13} \text{ K s}^{-1}$. The initial temperature profile is determined by the assumption of steady-state conditions with zero velocity. Temperature at the surface and the

bottom of the thermal boundary layer are fixed at 750 K and at a value T_{bl} taken as free parameter.

The phase diagram is assumed to be that of tholeiitic basalt [13], and the densities of gabbro and eclogite are taken to be 2900 and 3500 kg m⁻³. The density of garnet-granulite is assumed to increase linearly from that of gabbro to that of eclogite as pressure increases at a given temperature. The density of the mantle is assumed to be 3400 kg m⁻³. The micromechanism of the gabbro-eclogite transition is not well understood. In this study we assume that the volume diffusion of cations is the most likely rate-limiting process of the transformation, which involves chemical as well as phase changes. The volume fraction of reacted component, Ψ , is given by

$$\dot{\Psi}\Psi = D/r^2$$

where r is the grain radius and D is the diffusion coefficient [12]. Since the slowest-moving cation limits the reaction rate and Al³⁺ is likely to be this cation, we adopt as a minimum value for D the lower end of the range of estimates of the diffusion rate of Al³⁺ in orthopyroxene [14]

$$D = D_{Al,Opx} = 1.1 \times 10^{-5} \exp(-400 \text{ kJ}/RT)$$

where R is the gas constant and T is the absolute temperature. The diffusion rate, however, is experimentally uncertain because Al³⁺ diffusion is extremely sluggish, particularly at low temperature. In order to bound D from above, we use the diffusion rate of Fe in garnet ($D_{Fe,Gt} = 6.4 \times 10^{-8} \exp[-(270 \text{ kJ} + 5.7 \times 10^{-5} P)/RT]$), where P is in Pa. For each parcel of shortening lithosphere, Ψ is obtained by integration over time. The density at a given depth is determined from the volume fractions of unreacted and reacted components.

Numerical Results: Temperatures in the thickening crust and mantle are calculated for rates of horizontal convergence of 10⁻¹⁵ (Fig. 1a) and 10⁻¹⁶ s⁻¹ (Fig. 1b). For all models discussed here (Table 1), thicknesses of crust and thermal boundary layer are assumed to be initially 20 and 50 km, respectively, and to increase to 100 and 250 km, respectively. Temperature profiles for the strain rate of 10⁻¹⁵ s⁻¹ are vertically stretched as the crust and lithospheric mantle are thickened (Fig. 1a). Temperatures do not increase significantly from initial values because heat is mainly transferred by advection and the contribution of crustal heat production is minor. Hence gabbro remains metastable for 50 m.y. or more, and

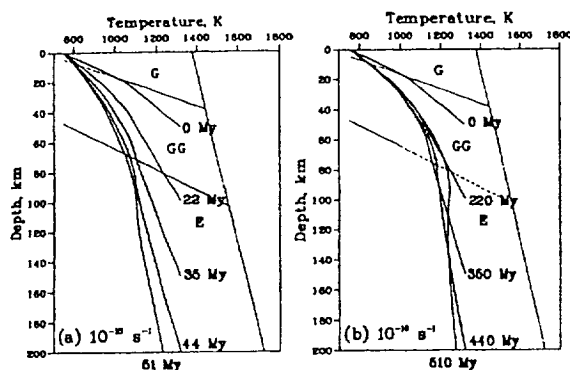


Fig. 1. Thermal evolution of crust and mantle thickened by a uniform horizontal strain rate of (a) 10⁻¹⁵ and (b) 10⁻¹⁶ s⁻¹. The phase diagram of the gabbro (G)—garnet granulite (GG)—eclogite (E) transition [13] is also shown. The models shown correspond to models (a) 1, 2, and 3, and (b) 4, 5, and 8 in Table 1.

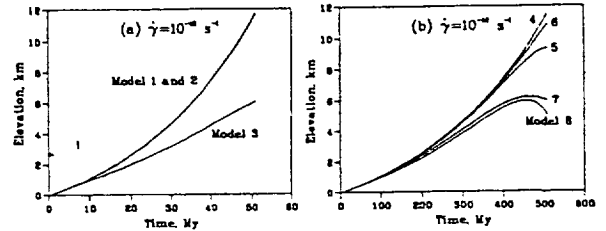


Fig. 2. Temporal variations of elevation for the models in Table 1.

the elevation of shortened lithosphere can increase as much as 12 km above the surrounding plains in that time interval (Fig. 2a). The phase transition proceeds, i.e., elevation is limited, only if grains are small and diffusion is fast (Model 3).

For $\dot{\gamma} = 10^{-16}$ s⁻¹, crustal heat production dominates advective heat transfer after the crust becomes as thick as 60–80 km (Fig. 1b). The resulting increase in temperature hastens the phase transition. The slower strain rate also lengthens the formation time of the mountains relative to the characteristic reaction time, which depends on r , D , and temperature at the base of the crust. For larger grains ($r = 10$ mm), the elevation reaches 11 km or more if the initial temperature at the base of the crust, T_c , is 1150 K (Model 6 in Fig. 2b). For the same value of T_c the elevation is at most 6 km for grains of 1-mm radius (Model 7). This result constitutes an upper bound on T_c for small grain size. If $D = D_{Fe,Gt}$ is assumed, that upper bound is lowered to 1050 K (Model 8).

Discussion: Because at long wavelengths the topography of western Ishtar Terra is correlated with the gravity field, dynamical support of the broad 4-km elevation of the region is likely [e.g., 15]. Therefore, the 7-km elevation of Maxwell Montes above the adjacent plateau is a more meaningful constraint on maximum relief than the 11-km elevation above mean planetary radius. The results are insensitive to the assumed initial thickness of crust but are sensitive to the density difference between crust and mantle. If densities of 3000 and 3300 kg m⁻³ for crust and mantle are assumed, elevations are 40% lower than the values presented here. Such changes constrain the models of thermal structure and phase transition depth more severely at low strain rate than the density values adopted above.

Two diffusion rates have been assumed in this study so as to represent a wide range of diffusion data. We should note, however, that under wet conditions, i.e., in the presence of either water [16] or melt [17], grain-boundary diffusion becomes much more efficient than volume diffusion. This is potentially noteworthy for understanding the contrast between Maxwell and Danu Montes. Despite the fact that Danu Montes display compressional deformation as extensive as the other mountain belts, the maximum elevation is as little as 0 km above the bounding plateau. Such comparatively modest elevation may be related to the presence of magmatic features within Danu Montes, if elevation is limited by an enhanced diffusion rate because of the melt at grain boundaries. Assessing the cause of higher temperatures beneath Danu Montes requires more detailed thermal models than the simple one-dimensional model considered here.

Conclusions: Taking into account the temperature-dependent reaction rate of the gabbro-eclogite phase transition, horizontal strain rates of 10⁻¹⁵ and 10⁻¹⁶ result in significant differences in the maximum elevation of mountains, not only because of the difference in the formation time for relief, but also because of the difference in the thermal regime from advection-dominated to

TABLE 1. Model parameters.

Models	r, mm	$\dot{\gamma}$, s ⁻¹	D	T _c , K	T _{bl} , K
1	1	10 ⁻¹⁵	D _{Al,Oppx}	1050	1321
2	10	10 ⁻¹⁵	D _{Al,Oppx}	1050	1321
3	1	10 ⁻¹⁵	D _{Fe,Gt}	1050	1321
4	1	10 ⁻¹⁶	D _{Al,Oppx}	1050	1321
5	10	10 ⁻¹⁶	D _{Al,Oppx}	1050	1321
6	10	10 ⁻¹⁶	D _{Al,Oppx}	1350	1521
7	1	10 ⁻¹⁶	D _{Al,Oppx}	1150	1521
8	10	10 ⁻¹⁶	D _{Fe,Gt}	1050	1321

crustal-heat-production dominated. For $\dot{\gamma} = 10^{-15} \text{ s}^{-1}$, the observed maximum elevation of mountain belts can be explained as a consequence of disequilibrium phase boundary depth for a wide range of physical parameters, although a comparatively young age for Maxwell Montes (50 m.y.) is implied. For the lesser horizontal strain rate of 10^{-16} s^{-1} , only limited parameter values for thermal models are allowed.

References: [1] Barsukov V. L. et al. (1986) *Proc. LPSC 16th*, in *JGR*, 91, D378. [2] Solomon S. C. et al. (1991) *Science*, 252, 297. [3] Head J. W. et al. (1991) *Science*, 252, 276. [4] Pronin A. A. (1986) *Geotectonics*, 20, 271. [5] Basilevsky A. T. (1986) *Geotectonics*, 20, 282. [6] Grimm R. E. and Phillips R. J. (1990) *GRL*, 17, 1349. [7] Roberts K. M. and Head J. W. (1990) *GRL*, 17, 1341. [8] Bindschadler D. L. and Parmentier E. M. (1990) *JGR*, 95, 21329. [9] Crumpler L. S. et al. (1986) *Geology*, 14, 1031. [10] Surkov Yu. A. et al. (1987) *Proc. LPSC 17th*, in *JGR*, 92, E537. [11] Vorder Bruegge R. W. and Head J. W. (1991) *Geology*, 19, 885. [12] Ahrens T. J. and Schubert G. (1975) *Rev. Geophys. Space Phys.*, 13, 383. [13] Ito K. and Kennedy G. C. (1971) *Geophys. Mon.*, 14, 303. [14] Smith D. and Barron B. R. (1991) *Am. Mineral.*, 76, 1950. [15] Grimm R. E. and Phillips R. J. (1991) *JGR*, 96, 8305. [16] Joesten R. (1991) In *Diffusion, Atomic Ordering and Mass Transport*, 345, Springer-Verlag. [17] Condit R. H. et al. (1985) *Geophys. Mon.*, 31, 97.

N93-14351

RESULTS OF A ZONALLY TRUNCATED THREE-DIMENSIONAL MODEL OF THE VENUS MIDDLE ATMOSPHERE. M. Newman, CIRES, University of Colorado, Boulder CO 80309, USA.

Although the equatorial rotational speed of the solid surface of Venus is only 4 m s^{-1} , the atmospheric rotational speed reaches a maximum of approximately 100 m s^{-1} near the equatorial cloud top level (65 to 70 km). This phenomenon, known as superrotation, is the central dynamical problem of the Venus atmosphere. We report here the results of numerical simulations aimed at clarifying the mechanism for maintaining the equatorial cloud top rotation.

Maintenance of an equatorial rotational speed maximum above the surface requires waves or eddies that systematically transport angular momentum against its zonal mean gradient. The zonally symmetric Hadley circulation is driven thermally and acts to reduce the rotational speed at the equatorial cloud top level; thus wave or eddy transport must counter this tendency as well as friction. Planetary waves arising from horizontal shear instability of the zonal flow (barotropic instability) could maintain the equatorial rotation by transporting angular momentum horizontally from midlatitudes toward the equator. Alternatively, vertically propagating waves could provide the required momentum source. The

relative motion between the rotating atmosphere and the pattern of solar heating, which has a maximum where solar radiation is absorbed near the cloud tops, drives diurnal and semidiurnal thermal tides that propagate vertically away from the cloud top level. The effect of this wave propagation is to transport momentum toward the cloud top level at low latitudes and accelerate the mean zonal flow there.

We employ a semispectral primitive equation model with a zonal mean flow and zonal wavenumbers 1 and 2 [1]. These waves correspond to the diurnal and semidiurnal tides, but they can also be excited by barotropic or baroclinic instability. Waves of higher wavenumbers and interactions between the waves are neglected. Symmetry about the equator is assumed, so the model applies to one hemisphere and covers the altitude range 30 to 110 km. Horizontal resolution is 1.5° latitude, and vertical resolution is 1.5 km. Solar and thermal infrared heating, based on Venus observations and calculations drive the model flow [2]. Dissipation is accomplished mainly by Rayleigh friction, chosen to produce strong dissipation above 85 km in order to absorb upward propagating waves and limit extreme flow velocities there, yet to give very weak Rayleigh friction below 70 km; results in the cloud layer do not appear to be sensitive to the Rayleigh friction. The model also has weak vertical diffusion, and very weak horizontal diffusion, which has a smoothing effect on the flow only at the two grid points nearest the pole.

Simulations were carried out with uniform background angular velocity equivalent to an equatorial speed of u_0 , where u_0 was varied between 50 and 75 m s^{-1} . Flow with this angular velocity was the initial condition for half of the simulations. The initial condition for the other half was obtained by adding to this background rotation a horizontally uniform, cyclostrophic-balanced component with zero additional zonal velocity at 30 and 110 km and a smooth increase to a maximum addition of 50 m s^{-1} at 65 km on the equator. Model runs were also carried out in which the coefficient of vertical diffusion ν was varied. Cases were run for 350 simulated (Earth) days, by which time a statistically steady state was reached. We present averages for the last 40 days of each run.

In the resulting mean zonal flow, the equilibrated equatorial wind maximum was typically between 90 and 105 m s^{-1} , and a jet developed near 40° latitude. The tides, particularly the semidiurnal tide, acted to balance (upgradient/downgradient) vertical advection by the Hadley cell updraft (below/above) the low-latitude zonal wind maximum. Experiments in which u_0 was varied indicated that the shape of this vertical jet (i.e., the vertical wind shear) is less sensitive to the background rotation than is the value of the speed maximum. This suggests that any theory that describes the role of the thermal tides in maintaining the equatorial rotational wind structure against vertical advection cannot oversimplify the vertical wind structure. Vertical diffusion acted to counter the tidal acceleration at cloud top, producing a slower zonal wind speed. For example, for two runs employing the sheared 60 m s^{-1} background rotation, reduction of ν from 2.5 to $1.0 \text{ m}^2 \text{ s}^{-1}$ produced an increase of more than 10 m s^{-1} in the equatorial zonal wind maximum. The diurnal tide transported angular momentum horizontally from the region of the midlatitude jet toward lower latitudes, acting to smooth the zonal wind profile between the midlatitude jets and the equator; thus, the jet does not become significantly barotropically unstable.

The tides also acted to weaken the Hadley circulation through both their meridional and upward heat fluxes. At the equator, the vertical convergence of the upward heat flux compensates part of the zonally averaged solar heating in the cloud top region. This effect reduced the mean equatorial cloud-level updraft by half, as compared to zonally symmetric model runs. Thus the tides act to